Dynamics of planar piecewise-smooth slow-fast systems

Glendinning, P and Kowalczyk, P

2010

MIMS EPrint: **2010.44**

ISSN 1749-9097

Dynamics of planar piecewise-smooth slow-fast systems

P. Glendinning [a] and P. Kowalczyk [b,*]

[a] *School of Mathematics and Centre for Interdisciplinary Computational and Dynamical Analysis (CICADA), University of Manchester, Manchester, M13 9PL, U.K.*

[b] *Centre for Interdisciplinary Computational and Dynamical Analysis (CICADA), University of Manchester, Manchester, M13 9PL, U.K.*

Abstract

In the paper we study the qualitative dynamics of piecewise-smooth slow-fast systems (singularly perturbed systems). First we consider in detail a planar system when the slow and the fast dynamics are one-dimensional. The slow manifold of the reduced system is a piecewise continuous curve – differentiability is lost across the switching surface. We show that in the full system the slow manifold is no longer continuous across the switching surface. There is an $\mathcal{O}(\varepsilon)$ discontinuity across the switching manifold. However, this discontinuity cannot qualitatively affect system dynamics. We show that system trajectories move across the switching surface and evolve exponentially fast toward the slow manifold that lies on the other side of the switching surface; small scale oscillations between the two parts of the slow manifold are not possible. We then classify the system dynamics in the case when there is an equilibrium on the switching surface. The results of our analysis are then used to investigate the dynamics of a simple box model of a climate change. The presence of a non-smooth equivalent of a fold bifurcation in the model is shown. Finally, the results on the topology of the slow manifolds across the switching surface are generalized to $n+1$-dimensional slow-fast systems (the slow dynamics being n-dimensional).

Key words: Non-smooth systems, singular perturbation, slow-fast dynamics

* Corresponding author.
Email address: piotr.kowalczyk@manchester.ac.uk (P. Kowalczyk).

1 Introduction

Many systems of relevance to applications are modeled using piecewise-smooth dynamical systems. Examples include systems modeled by a set of ordinary differential equations that lose their smoothness properties across co-dimension one manifolds in phase space. Applications include DC/DC power converters which are modeled using distinct sets of ordinary differential equations between which a converter switches depending on whether the switching element is in the on or off state [1]; friction oscillators [2–4], impacting systems [5–7] are other examples of applications which are modeled by systems with discontinuous nonlinearities.

Much research effort has recently been spent on understanding the qualitative dynamics of these systems and a theory of phase space transitions triggered by the presence of discontinuous nonlinearities has been developed [8–10]. These phase space transitions are termed discontinuity induced bifurcations, DIBs for short. At present there exists a fairly complete description of co-dimension one DIBs of limit cycles and equilibrium points. However, one of the pressing issues with regards to investigations of the dynamics of piecewise-smooth systems is the effect of stable singular perturbations. For sufficiently differentiable vector fields the theory developed by Tikhonov [11] and Fenichel [12] makes it possible to treat singular perturbation problems as regular perturbation problems by proving the existence of a hyperbolic invariant manifold. This is not the case when piecewise-smooth systems are treated. Due to the presence of the discontinuity a slow manifold usually exhibits a discontinuity across a surface (or hyper-surface) of phase space where the smoothness property of vector fields governing system equations are lost [13]. In this case - systems modeled by discontinuous vector fields (Filippov systems) - it was shown that when the switching between vector fields does not depend on the fast variable then a hyperbolic limit cycle that exists in the reduced system is also present in the full system and its stability properties are preserved.

However, the presence of the discontinuity may carry significant implications regarding system dynamics; Fenichel's theory reduces singular perturbations of smooth vector fields to regular ones by proving the existence of a hyperbolic smooth manifold which is approached exponentially fast by trajectories and hence qualitative studies of system dynamics can be conducted by considering the dynamics on the manifold. However, if the modeling results in a system that is piecewise-smooth then the slow manifold of the full system is discontinuous and Fenichel's theory cannot be applied. For instance, singularly perturbed planar Filippov systems may produce micro-chaotic dynamics [14]. This in turn carries practical implications: seemingly noisy output from an experiment may result from the fast dynamics neglected in the modeling procedure and be in fact of a deterministic nature. The knowledge of the effects of singular perturbations on system dynamics would then allow one to establish the 'size' of this neglected dynamics and provide more insight into the experiment. For these reasons it is necessary to complete the theory of piecewise-smooth systems by considering the effects of singular perturbations.

In our work we focus on a class of piecewise-smooth systems which are continuous in the phase space region of interest but the vector field Jacobians are discontinuous across a smooth manifold (*switching manifold*).

The paper is organized as follows. In Sec. 2 we introduce the planar slow-fast piecewise-smooth systems studied here. The slow and fast dynamics are one-dimensional. In Sec. 3 phase space topology, and in particular the topology of the slow manifold, of the reduced and full system is investigated. The difference between our approach and the work presented in [13] is that we consider smooth vector fields with discontinuous Jacobians and the switching depends on both the slow and fast variables. In [13] Filippov systems are investigated and the authors make additional assumption that the switching does not depend on the fast variable. This assumption though convenient for the analytical purposes may not be met in practice.

The discontinuity of the slow manifold in the full system is established and the size of the discontinuity is linked with the differentiability properties of the vector fields across the switching manifold. In Sec. 4 the qualitative dynamics of the reduced and full system is investigated in the special case that an equilibrium point exists on the switching surface. This is a natural co-dimension one bifurcation point, but we show that nothing surprising can be induced by the discontinuity. Then, in Sec. 5 a box model of a thermohaline circulation is analyzed. The model is a planar piecewise-smooth slow-fast system obtained by a novel scaling of an example due to [15].

We then use our results from previous sections to analyze the dynamics of the model. In particular, the presence of a non-smooth equivalent of a fold bifurcation is explained. In Sec. 6 we extend our investigations to $n+1$ dimensional slow-fast piecewise-smooth systems where the slow dynamics is $n-$dimensional. We show that the character of the discontinuity of the slow manifold across the switching surface generalizes to higher dimensional systems. Finally in Sec. 7 we conclude the paper highlighting open problems and indicating further directions for the theory of singularly perturbed piecewise-smooth systems.

2 Switched slow-fast systems

Consider slow-fast systems of the form

$$\dot{y} = \begin{cases} g_+(x, y; \varepsilon) & \text{if } h(x, y) \geq 0, \\ g_-(x, y; \varepsilon) & \text{if } h(x, y) < 0, \end{cases} \tag{1}$$

$$\varepsilon \dot{x} = \begin{cases} f_+(x, y;\, \varepsilon) & \text{if } h(x, y) \geq 0, \\ f_-(x, y;\, \varepsilon) & \text{if } h(x, y) < 0, \end{cases} \tag{2}$$

where $x \in \mathbb{R}$, $y \in \mathbb{R}$, and $\varepsilon > 0$ is a small parameter measuring the difference in the time scale between the evolution of fast (x) and slow variables (y). Assume that $f_\pm$, $g_\pm : \mathbb{R}^2 \times \mathbb{R} \mapsto \mathbb{R}$ are sufficiently differentiable functions of x, y and ε, well defined for all (x, y) in a region of interest. The zero-level set of function $h : \mathbb{R}^2 \mapsto \mathbb{R}$ defines the switching surface, Σ, i.e.

$$\Sigma := \{(x,\, y) \in \mathbb{R}^2 : h(x,\ y) = 0\}.$$

Note that h is independent of ε. We assume that $f_- = f_+$, and $g_- = g_+$ for $(x,\, y) \in \Sigma$ but $\nabla f_+ \neq \nabla f_-$ and $\nabla g_+ \neq \nabla g_-$ on Σ, where '∇' denotes the gradient differential operator. In what follows we will also use the notation $\nabla f_\pm = [f_{\pm x},\, f_{\pm y}]$ and $\nabla g_\pm = [g_{\pm x},\, g_{\pm y}]$, where subscripts '$x$' and '$y$' denote partial differentiation with respect to 'x' and 'y' variables.

Furthermore, define regions where the system dynamics is smooth and governed by the slow-fast systems $(f_+,\, g_+)$ and $(f_-,\, g_-)$ respectively, as

$$G_+ := \{(x,\, y) \in \mathbb{R}^2 : h(x,\ y) > 0\},$$

$$G_- := \{(x,\, y) \in \mathbb{R}^2 : h(x,\ y) < 0\}.$$

We assume further that for $\varepsilon = 0$ the nonlinear equations $f_\pm(x,\, y;\, 0) = 0$ can be solved for x for all y giving $x^0_\pm(y)$ respectively. We also assume the stability condition

$$0 > -c > \text{Re } D_x f_\pm(x^0_\pm(y), y; 0), \qquad \forall y, \tag{3}$$

where D_x denotes differentiation with respect to x variable, and c is a positive constant. The first of these two assumptions is guaranteed provided that the Implicit Function Theorem can be applied for all $(x,\, y)$ to find $x^0_\pm(y)$ in the region of interest, and the second of these is the standard condition for the application of Fenichel Theory [12].

3 Phase space topology

3.1 General description

Let us first consider phase space topology of (1) and (2) when $\varepsilon = 0$. Relations $f_\pm(x, y, 0) = 0$ define smooth manifolds, say $\mathcal{M}_+$ in G_+ and $\mathcal{M}_-$ in G_- respectively. Let $(x(y_-^*),\ y_-^*)$ and $(x(y_+^*), y_+^*)$ be the points of intersection of $\mathcal{M}_-$ and $\mathcal{M}_+$ with Σ, respectively. There exists only one point $(x(y^*),\ y^*) \in \Sigma$ such that $f_+^0(x(y^*),\ y^*; 0) = 0$ and $f_-^0(x(y^*),\ y^*; 0) = 0$. Hence, $(x(y_-^*),\ y_-^*) = (x(y_+^*), y_+^*)$ and $\mathcal{M}_+, \mathcal{M}_-$ intersect on Σ. We made an implicit assumption here that $\mathcal{M}_\pm$ are transversal to Σ at $(x(y_-^*),\ y_-^*) = (x(y_+^*), y_+^*)$ i.e. $\langle \nabla h, \nabla f_\pm^0 \rangle \neq 0$ on Σ, which can be assumed without loss of generality ($\langle\ ,\ \rangle$ denotes the dot product). In this notation ∇h is a vector normal to Σ and $\nabla f_\pm^0$ is a vector normal to $\{f_\pm^0(x(y),\ y) = 0\}$ respectively.

In this setting we define the reduced system that lives on $\mathcal{M}_- \cup \mathcal{M}_+$ as

$$\dot{y} = \begin{cases} g_+(x_+^0(y), y;\ 0) & \text{if } h(x, y) \geq 0, \\ g_-(x_-^0(y), y;\ 0) & \text{if } h(x, y) < 0. \end{cases} \tag{4}$$

Clearly, the reduced system (4) evolves on a piecewise continuous slow manifold $\mathcal{M} = \mathcal{M}_+ \cup \mathcal{M}_-$. Consider now how the structure of phase space changes for $\varepsilon > 0$.

In each of the regions G_+ and G_- there exist invariant manifolds, say $\mathcal{M}_+^\varepsilon$ and $\mathcal{M}_-^\varepsilon$ respectively, consisting of all trajectories (in our case it is one trajectory) without rapidly decaying fast parts. By the continuity argument these manifolds are $\mathcal{O}(\varepsilon)$ perturbations of $\mathcal{M}_+$ and $\mathcal{M}_-$. It is important to determine if these manifolds create a continuous manifold, say $\mathcal{M}^\varepsilon = \mathcal{M}_+^\varepsilon \cup \mathcal{M}_-^\varepsilon$ defined in the whole phase space of interest.

We assume that the slow manifold $\mathcal{M}_+^\varepsilon$ can be expressed as a power series in ε, i.e.

$$x_+(y) = \alpha_0(y) + \varepsilon\alpha_1(y) + \mathcal{O}(\varepsilon^2) \tag{5}$$

and its coefficients are such that (5) solves (2) for $\varepsilon > 0$; obviously $\alpha_0(y),\ \alpha_1(y),\ \cdots$, are coefficients (functions of the slow variable y) to be determined. Differentiating $x_+(y)$, term by term, with respect to t gives

$$\dot{x}_+(y) = \alpha_0'(y)\dot{y} + \varepsilon\alpha_1'(y)\dot{y} + \mathcal{O}(\varepsilon^2), \tag{6}$$

where the '$\prime$' symbol denotes differentiation with respect to y.

The slow manifold $\mathcal{M}_-^\varepsilon$ can then be given by an equivalent functional expression

$$x_-(y) = \beta_0(y) + \varepsilon\beta_1(y) + \mathcal{O}(\varepsilon^2). \tag{7}$$

Differentiating $x_-(y)$ term by term gives

$$\dot{x}_-(y) = \beta_0'(y)\dot{y} + \varepsilon\beta_1'(y)\dot{y} + \mathcal{O}(\varepsilon^2), \tag{8}$$

where again $\beta_0(y)$, $\beta_1(y)$, $\cdots$, are coefficients (functions of the slow variable y) to be determined. Let us express $f_\pm(x,\, y;\, \varepsilon)$ and $g_\pm(x,\, y;\, \varepsilon)$ as power series in ε. We then have

$$f_\pm(x,\, y;\, \varepsilon) = f_\pm^{(0)}(x, y) + \varepsilon f_\pm^{(1)}(x, y) + \mathcal{O}(\varepsilon^2), \tag{9}$$

and

$$g_\pm(x,\, y;\, \varepsilon) = g_\pm^{(0)}(x, y) + \varepsilon g_\pm^{(1)}(x, y) + \mathcal{O}(\varepsilon^2), \tag{10}$$

where $f_\pm^{(0)}(x, y) \equiv f_\pm(x, y;\, 0)$. We can now use (1), (2), and (5)-(9) to determine α_0, α_1, β_0, and β_1.

Consider first $\mathcal{O}(1)$ terms of (2) when the left-hand side of (2) is 0, that is when $\varepsilon = 0$. Substituting into the right-hand side of (2), equation (9), we have that the $\mathcal{O}(1)$ term can be defined through

$$f_\pm^{(0)}(x, y) = 0. \tag{11}$$

Under our initial assumption that the Implicit Function Theorem (IFT) can be applied for all $(x,\, y)$ in the region of interest to find $x_\pm^0(y)$, we can find $\alpha_0(y)$, and $\beta_0(y)$. Note that $\alpha_0(y) \equiv x_+^0(y)$ and $\beta_0(y) \equiv x_-^0(y)$. In other words the leading order terms that give functional expressions for the slow manifolds $\mathcal{M}_\pm^\varepsilon$ of the full system reduce to those that determine the slow manifolds $\mathcal{M}_\pm$ of the reduced system (4).

Note in particular that as (11) holds for all y in $h(x,\, y) \leq 0$ and $h(x,\, y) > 0$,

$$\frac{d}{dy}(f_+^{(0)}(\alpha_0(y), y)) = 0. \quad \text{Hence} \quad f_{+x}^{(0)}(\alpha_0, y)\alpha_0'(y) + f_{+y}^{(0)}(\alpha_0, y) = 0,$$

which gives

$$\alpha_0'(y) = -\frac{f_{+y}^{(0)}}{f_{+x}^{(0)}} \tag{12}$$

and is well defined provided that $f_{+x}^{(0)} \neq 0$, and similarly

$$\beta_0'(y) = -\frac{f_{-y}^{(0)}}{f_{-x}^{(0)}} \tag{13}$$

and is well defined provided that $f_{-x}^{(0)} \neq 0$. It then follows that

$$\alpha_0'(y) \neq \beta_0'(y) \Leftrightarrow f_{+x}^0 f_{-y}^0 - f_{+y}^0 f_{-x}^0 \neq 0. \tag{14}$$

We now compute terms of $\mathcal{O}(\varepsilon)$. Collecting terms of $\mathcal{O}(\varepsilon)$ from (2) we have that

$$\alpha_0'(y)g_+^{(0)}(\alpha_0, y) = \alpha_1(y)f_{+x}^{(0)}(\alpha_0, y) + f_+^{(1)}(\alpha_0, y). \tag{15}$$

Substituting (12) for α_0 into (15), we can rewrite (15) to get

$$\alpha_1(y) = \frac{-1}{[f_{+x}^{(0)}]^2}\left(f_{+y}^{(0)}g_+^{(0)} + f_+^{(1)}f_{+x}^{(0)}\right) \tag{16}$$

with the quantities on the right-hand side of (16) evaluated at (α_0, y). Similarly we find that $\beta_1(y)$ is given by

$$\beta_1(y) = \frac{-1}{[f_{-x}^{(0)}]^2}\left(f_{-y}^{(0)}g_-^{(0)} + f_-^{(1)}f_{-x}^{(0)}\right). \tag{17}$$

We now wish to determine if $x_+(y)$ and $x_-(y)$ are continuous on Σ.

Suppose that $(x_-(y_-^{in}),\ y_-^{in})$ and $(x_+(y_+^{in}),\ y_+^{in})$ are the points of intersection of $\mathcal{M}_-^\varepsilon$ and $\mathcal{M}_+^\varepsilon$ with Σ respectively, and that Σ is defined by the equation $h(x,y) = 0$, with no ε dependence (although such dependence could easily be treated). Recall that $\mathcal{M}_-^0$ and $\mathcal{M}_+^0$ intersect Σ at the same point, with $y-$coordinate y^*. Thus we are looking to find the order ε terms for the intersection points, and we can expand

$$y_\pm^{in} = y^* + \varepsilon y_{\pm 1}^* + \mathcal{O}(\varepsilon^2). \tag{18}$$

and seek to find $y_{\pm 1}^*$ and the corresponding correction to the $x-$coordinates.

By definition

$$\begin{aligned} x_+(y_+^{in}) &= \alpha_0(y_+^{in}) + \alpha_1(y_+^{in})\varepsilon + \mathcal{O}(\varepsilon^2) \\ &= \alpha_0(y^* + \varepsilon y_{\pm 1}^*) + \alpha_1(y^*)\varepsilon + \mathcal{O}(\varepsilon^2) \\ &= \alpha_0(y^*) + \left(\alpha_0'(y^*)y_{\pm 1}^* + \alpha_1(y^*)\right)\varepsilon + \mathcal{O}(\varepsilon^2) \end{aligned} \tag{19}$$

and so $h(x_+(y_+^{in}), (y_+^{in})) = 0$ becomes (retaining only terms up to order ε)

$$h(x^*,\, y^*) + \left(h_x^*\alpha_0'(y^*)y_{+1}^* + \alpha_1(y^*)) + h_y^* y_{+1}^*\right)\varepsilon = 0, \tag{20}$$

where starred functions are evaluated at $(\alpha_0(y^*), y^*)$. The first term is zero by the definition of y^*, and so setting the ε term to zero gives

$$y_{+1}^* = -\frac{h_x^*\alpha_1(y^*)}{h_x^*\alpha_0'(y^*) + h_y} \tag{21}$$

provided $h_x\alpha_0'(y^*) + h_y \neq 0$, or, using (12),

$$y^*_{+1} = -\frac{h^*_x f^{(0)*}_{+x}\alpha_1(y^*)}{h^*_y f^{(0)*}_{+x} - h^*_x f^{(0)*}_{+y}} = -\frac{f^{(0)*}_{+x}\alpha_1(y^*)}{\frac{h^*_y}{h^*_x} f^{(0)*}_{+x} - f^{(0)*}_{+y}} \tag{22}$$

with α_1 given by (16). Now, if the boundary Σ is written in the form $x = b(y)$ then $h(b(y), y) = 0$ implies that $b'(y) = -h_y/h_x$ by the same argument which showed (12). But since f is continuous across Σ then $f^{(0)}_+(b(y), y) - f^{(0)}_-(b(y), y) = 0$ and so the same argument implies that $b'(y) = -(f^{(0)}_{+y} - f^{(0)}_{-y})/(f^{(0)}_{+x} - f^{(0)}_{-x})$ on the boundary, and so putting these two equations for $b'(y)$ together we obtain

$$\frac{h_y}{h_x} = \frac{(f^{(0)}_{+y} - f^{(0)}_{-y})}{(f^{(0)}_{+x} - f^{(0)}_{-x})} \tag{23}$$

on the boundary Σ. This allows us to replace the ratio h_y/h_x in the lowest order expansion by the right hand side of (23) evaluated at y^*, which after a little tidying up using (16) gives

$$y^*_{+1} = \frac{(f^{(0)}_{+x} - f^{(0)}_{-x})(g^{(0)}_+ f^{(0)}_{+y} + f^{(1)}_+ f^{(0)}_{+x})}{f^{(0)}_{+x}(f^{(0)}_{-x} f^{(0)}_{+y} - f^{(0)}_{-y} f^{(0)}_{+x})}. \tag{24}$$

A precisely analogous argument yields

$$y^*_{-1} = \frac{(f^{(0)}_{+x} - f^{(0)}_{-x})(g^{(0)}_- f^{(0)}_{-y} + f^{(1)}_- f^{(0)}_{-x})}{f^{(0)}_{-x}(f^{(0)}_{-x} f^{(0)}_{+y} - f^{(0)}_{-y} f^{(0)}_{+x})}. \tag{25}$$

Thus $y^*_{+1} \neq y^*_{-1}$ in general, so $\mathcal{M}^\varepsilon$ is discontinuous across Σ and the size of the discontinuity is $\mathcal{O}(\varepsilon)$. The discontinuity is triggered by the non-differentiability of the slow manifold of the reduced system. Note that $x_+(y^{in}_+)$ can be calculated from (24) and (19), with an analogous result for $x_-(y^{in}_-)$.

3.2 Equilibrium of the reduced system on Σ

In Sec. 4.2 we consider the case when the reduced system exhibits an equilibrium, which we denote as $(\alpha_0(y^*),\, y^*)$, on the switching manifold, i.e.

$$g^{(0)}_\pm(\alpha_0(y^*), y^*) = 0. \tag{26}$$

In this case we need to check whether the general conclusions of the previous section still hold. Note that (24) and (25) hold when $g^{(0)}_\pm = 0$, so

$$y^*_{\pm 1} = \frac{f^{(1)}_\pm (f^{(0)}_{+x} - f^{(0)}_{-x})}{(f^{(0)}_{-x} f^{(0)}_{+y} - f^{(0)}_{-y} f^{(0)}_{+x})} \tag{27}$$

with the functions on the right hand side evaluated at $(x(y^*),\, y^*)$. But since $f_-^{(1)} \neq f_+^{(1)}$ in general (the order ε equation for the continuity of f across the boundary Σ contains terms from $f_\pm^{(0)}$) so the discontinuity of $\mathcal{M}_+^\varepsilon \cup \mathcal{M}_+^\varepsilon$ on Σ remains of order ε.

3.3 A local co-ordinate system

In Sec. 4.1 we consider the dynamics close to the switching surface and near the slow manifolds. To make the analysis as simple as possible it is natural to introduce a co-ordinate set in which the switching surface is given by $\{x = 0\}$ in terms of a new x variable. If (x^*, y^*) is the intersection of the slow manifolds for $\varepsilon = 0$ with the switching surface Σ then we assume that the equation

$$X = h(x, y) \tag{28}$$

can be inverted near (x^*, y^*) giving $x = H(X, y)$. This is possible provided $h_x(x, y) \neq 0$ in a neighbourhood of (x^*, y^*). Using (1) and (2) we find

$$\varepsilon \dot{X} = h_x f_\pm + \varepsilon h_y g_\pm \tag{29}$$

with the right hand side evaluated at $(H(X, y), y)$, and where the switching surface is now the set $\{X = 0\}$.

Defining $Y = y - y^*$ we obtain a new set of equations for which the intersection of the slow manifolds when $\varepsilon = 0$ is at $(X, Y) = (0, 0)$ and the switching surface has $X = 0$.

Without writing the new system in full detail we note that in these new coordinates the size of the discontinuity is again $\mathcal{O}(\varepsilon)$ for typical systems.

3.4 Special case

The box model for the climate change that we study in Sec. 5 is a special case of the planar slow-fast systems studied here; the function $f(x,\, y;\, 0)$ is at least C^1 differentiable $\forall (x,\, y)$ which implies that the slow manifold of the reduced system is a smooth curve across Σ. Thus, we will consider how the smoothness of the slow manifold affects system dynamics. Let us assume that the fast dynamics is given by

$$\varepsilon \dot{x} = f^{(0)}(x, y) + \begin{cases} \varepsilon f_+^{(1)}(x, y) + \varepsilon^2 f_+^{(2)}(x, y) + \mathcal{O}(\varepsilon^3) & \text{if } h(x, y) \geq 0, \\ \varepsilon f_-^{(1)}(x, y) + \varepsilon^2 f_-^{(2)}(x, y) + \mathcal{O}(\varepsilon^3) & \text{if } h(x, y) < 0, \end{cases} \tag{30}$$

where $f_+^{(1)} = f_-^{(1)}$ for (x, y) on Σ but $\nabla f_+^{(1)} \neq \nabla f_-^{(1)}$ (by the assumption on the continuity of the vector fields across the switching manifold the coefficients at all orders of ε are equal on Σ). In this setting, when we consider the reduced system, we note that the equation $f^{(0)}(x, y) = 0$ defines the slow manifold of the reduced system $\mathcal{M} = \mathcal{M}_+ \bigcup \mathcal{M}_-$, and $\mathcal{M}$ is a smooth curve across Σ by the fact that $f^{(0)}(x, y)$ is differentiable. Obviously under our initial assumption that the IFT can be applied for all $(x,\ y)$ in the region of interest to find $x_\pm^0(y)$, we find that $\alpha_0(y) \equiv x_+^0(y) \equiv \beta_0(y) \equiv x_-^0(y)$.

It might now appear from (24) and (25) that $y_{+1}^* = y_{-*}$, but a closer look at the derivation of (23) reveals that this relation uses $\nabla f_+^{(0)} \neq \nabla f_-^{(0)}$. This does not hold here, and so the correct leading order relation is

$$\frac{h_y}{h_x} = \frac{(f_{+y}^{(1)} - f_{-y}^{(1)})}{(f_{+x}^{(1)} - f_{-x}^{(1)})} \tag{31}$$

which can be substituted into (22) to find a new expression for y_{+1}^*, with an analogous argument giving a revised expression for y_{-1}^*. In general there is no reason for these to be equal and hence in general we expect the splitting of the manifolds to be first order in ε.

Indeed, this argument shows that that even if the splitting in f is $\mathcal{O}(\varepsilon^N)$, $N \geq 2$, then provided the splitting in g remains $\mathcal{O}(\varepsilon)$, the slow manifolds are separated by $\mathcal{O}(\varepsilon)$ on Σ.

4 Qualitative dynamics

In this section we will consider the dynamics of slow-fast system (1) and (2) at the point of intersection of the slow manifold $\mathcal{M}$ of the reduced system with the switching surface. Away from this point Fenichel's theory holds and standard results can be applied to study system dynamics. Let us assume that the switching surface is given by $\Sigma := \{h(x, y) = x = 0\}$, and the slow manifold $\mathcal{M}$ of the reduced system crosses Σ at the origin as described in Section 3.3.

4.1 Case I: No-equilibrium of the reduced system on the switching surface

We will begin by expanding $f_\pm$ about the origin and use this to unfold the dynamics of the full slow-fast system around the origin. Thus, the slow system which we shall study is left unchanged except for the switching surface, i.e.

we have

$$\dot{y} = \begin{cases} g_+(x, y; \varepsilon) & \text{if } x \geq 0, \\ g_-(x, y; \varepsilon) & \text{if } x < 0, \end{cases} \tag{32}$$

and the fast system becomes

$$\varepsilon \dot{x} = \begin{cases} -C_+ x + By + \varepsilon D + \mathcal{O}(||x, y, \varepsilon||^2) & \text{if } x \geq 0, \\ -C_- x + By + \varepsilon D + \mathcal{O}(||x, y, \varepsilon||^2) & \text{if } x < 0, \end{cases} \tag{33}$$

where $C_+ > 0$ and $C_- > 0$ and we can choose B to be positive or negative in the subsequent qualitative analysis. Without loss of generality we choose to consider positive B (negative B implies change of the direction of the flow on the slow manifold of the reduced system but the subsequent analysis can be conducted in like manner).

The form of the fast subsystem is the result of the continuity across Σ and the sign of C_+ and C_- being positive is determined by the fact that we consider stable singular perturbations (see Eq. 3), that is, all trajectories away from the slow manifold approach it exponentially fast. Thus setting $\varepsilon = 0$ in (33) gives the slow manifold of the reduced system as the union of $\mathcal{M}_+ := \{x_1 = BC_+^{-1} y\}$ and $\mathcal{M}_- := \{x_2 = BC_-^{-1} y\}$. Note that both $\mathcal{M}_+$ and $\mathcal{M}_-$ exist in the whole phase space $G_+ \cup \Sigma \cup G_-$ but we are only considering these parts which pertain to their domains of definition. Clearly $\mathcal{M}$ locally around the origin is a piecewise linear manifold. Let us assume that at the origin $\dot{y}(0) > 0$. Then on the slow manifold $\mathcal{M}$, $\dot{x}(0_-) = BC_-^{-1}\dot{y}(0) > 0$ and $\dot{x}(0_+) = BC_+^{-1}\dot{y}(0) > 0$. Thus in the reduced system, locally around the origin the trajectory crossing Σ exhibits a corner along its evolution and moves on $\mathcal{M}$ towards increasing values of x and y. Note that considering negative B in (33) implies the evolution to the left across Σ along the decreasing values of x.

Let us now consider the dynamics of the full system locally around the origin. Assume $C_+ > C_- > 0$. Then $B/C_- > B/C_+ > 0$. Functions $g_\pm(0, 0, \varepsilon) = a > 0$ for ε sufficiently small. Let us determine approximate expressions that define slow manifolds $\mathcal{M}_+^\varepsilon$ and $\mathcal{M}_-^\varepsilon$ about the origin. We use the power series expansions as explained in the former section. Thus, $\mathcal{M}_\pm^\varepsilon$ are approximately defined by the relations $x_+(y) = \alpha_0 + \varepsilon\alpha_1$ and $x_-(y) = \beta_0 + \varepsilon\beta_1$ respectively, where α_0, α_1, β_0, β_1 are coefficients to be determined. The coefficients α_0 and β_0 are obviously the functional expressions for the slow manifolds of the reduced system, and are given by $\alpha_0 = BC_+^{-1}y$ and $\beta_0 = BC_-^{-1}y$ respectively.

We use (16) and (17) to find α_1 and β_1 respectively. We have $f_{+x}^{(0)} = -C_+$, $f_{+y}^{(0)} = B$, $f_+^{(1)} = D$ $f_{-x}^{(0)} = -C_-$, $f_{-y}^{(0)} = B$, $f_-^{(1)} = D$ and $g_\pm^{(0)} = a$. We then obtain $\alpha_1 = -(BC_+^{-2}a - DC_+^{-1})\varepsilon$ and $\beta_1 = -(BC_-^{-2}a - DC_-^{-1})\varepsilon$. Thus, the approximate expressions for the slow manifolds can be given by

$$x_+(y) = BC_+^{-1}y - BC_+^{-2}a\varepsilon + DC_+^{-1}\varepsilon, \text{ and } x_-(y) = BC_-^{-1}y - BC_-^{-2}a\varepsilon + DC_-^{-1}\varepsilon. \tag{34}$$

The slow manifold $\mathcal{M}_+^\varepsilon$ crosses Σ at $(C_+^{-1}a + B^{-1}D)\varepsilon$, and the slow manifold $\mathcal{M}_-^\varepsilon$ crosses Σ at $(C_-^{-1}a + B^{-1}D)\varepsilon$. Note that $C_-^{-1}a\varepsilon > C_+^{-1}a\varepsilon > 0$. Thus $\mathcal{M}_+$ crosses the switching surface below $\mathcal{M}_-$ and the direction of the flow at the intersection points of $\mathcal{M}_\pm$ with Σ are $\dot{x}(y_+) = BC_+^{-1}a > 0$ and $\dot{x}(y_-) = BC_-^{-1}a > 0$ respectively.

4.2 Case II: Equilibrium of the reduced system on the switching surface

Consider now the situation when $g_\pm(0, 0, 0) = 0$, that is, the reduced system exhibits an equilibrium at the origin. We want to determine what is the dynamics of the slow fast system (32) and (33) around the origin in this case. Expanding (32) in x, y and ε to leading order yields

$$\dot{y} = \begin{cases} c_+x + by + d\varepsilon + \mathcal{O}(||x, y, \varepsilon||^2) & x \geq 0, \\ c_-x + by + d\varepsilon + \mathcal{O}(||x, y, \varepsilon||^2) & \text{if } x < 0. \end{cases} \tag{35}$$

In the current case the dynamics of the reduced system (33) and (35) about the origin is characterized by four qualitatively distinct phase portraits. The slow manifolds of the reduced system are given by the same functional expressions as in the previous case, namely $x_\pm = BC_\pm^{-1}y$. Thus the dynamics of the reduced system about the origin will depend on the signs of $\dot{x}$, and $\dot{y}$, for x and y about the origin. About the origin on the slow manifolds $\dot{x} = BC_\pm^{-1}(c_\pm BC_\pm^{-1} + b)y$ and $\dot{y} = (c_\pm BC_\pm^{-1} + b)y$. Clearly the aforementioned four cases depend on the signs of $(c_\pm BC_\pm^{-1} + b)$.

- Case I, $c_+BC_+^{-1} + b > 0$ and $c_-BC_-^{-1} + b > 0$. The origin is a repeller and for $x > 0$ the trajectory moves to the right, and for $x < 0$ the trajectory evolves to the left, away from the origin (See Fig. 1 (a)).
- Case II, $c_+BC_+^{-1} + b > 0$ and $c_-BC_-^{-1} + b < 0$. The origin is a saddle and for $x > 0$ the trajectory moves away from the origin, and for $x < 0$ the trajectory evolves toward the origin (See Fig. 1 (b)).
- Case III, $c_+BC_+^{-1}+b < 0$ and $c_-BC_-^{-1}+b < 0$. The origin is an attractor and for $x > 0$ the trajectory moves to the left toward the origin and similarly for $x < 0$ the trajectory also evolves toward the origin but along the increasing x (See Fig. 1 (c)).
- Case IV, $c_+BC_+^{-1} + b < 0$ and $c_-BC_-^{-1} + b > 0$. The origin is a saddle and for $x > 0$ the trajectory moves toward the origin, and for $x < 0$ the trajectory evolves away from the origin (See Fig. 1 (d)).

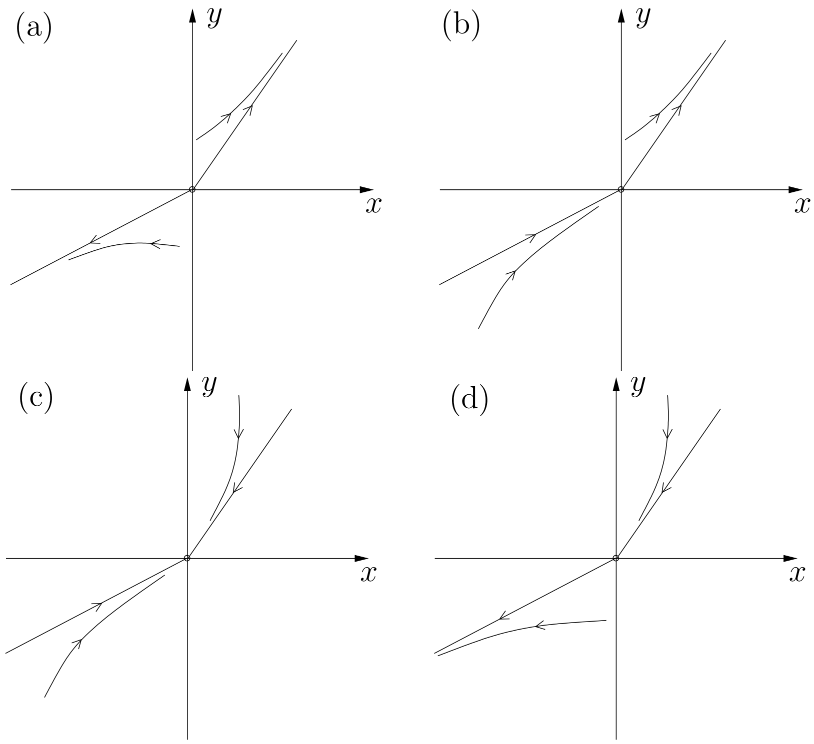

Fig. 1. Phase portraits of the reduced system (33) and (35) about the origin for $\varepsilon = 0$; (a) Case I with the origin being a repeller of the reduced system, (b) Case II with the origin a saddle node of the reduced system, (c) Case III with the origin an attractor of the reduced system, and (d) Case IV with the origin a saddle node of the reduced system.

We will now investigate the qualitative dynamics of (33) and (35) about the origin pertaining to the above four cases for $\varepsilon > 0$. To this aim we first determine where lie the equilibrium points of (33) and (35).

To leading order we find

$$\begin{aligned}(x_+^*,\, y_+^*) &= \left(\frac{-C_+^{-1}Bd\varepsilon}{c_+C_+^{-1}B+b},\ \frac{-d\varepsilon}{c_+C_+^{-1}B+b}\right),\\ (x_-^*,\, y_-^*) &= \left(\frac{-C_-^{-1}Bd\varepsilon}{c_-C_-^{-1}B+b},\ \frac{-d\varepsilon}{c_-C_-^{-1}B+b}\right).\end{aligned} \tag{36}$$

The equilibrium $(x_+^*,\, y_+^*)$ is an admissible equilibrium of our system if it exists for $x > 0$ otherwise it is a virtual equilibrium. Similarly $(x_-^*,\, y_-^*)$ is an admissible equilibrium of our system if it exists for $x < 0$ otherwise it is a virtual equilibrium.

In principle there is a possibility that switching ε to a positive value gives rise to three distinct qualitative dynamics for each of the four cases enumerated in the previous section. Namely, we would expect to observe:

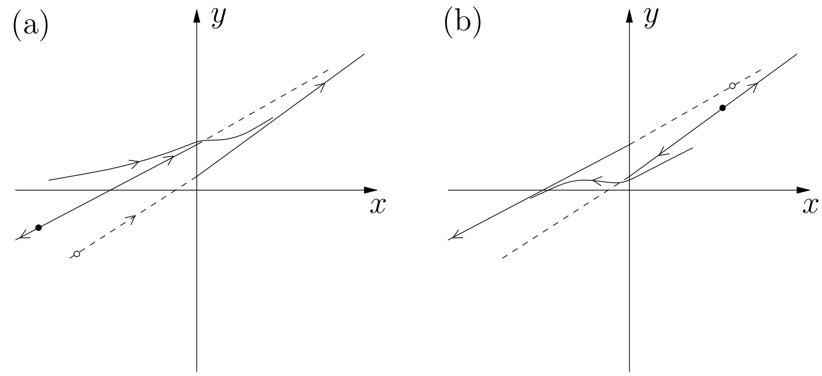

Fig. 2. Phase portraits of the slow fast system (33) and (35) about the origin for $\varepsilon > 0$ in the case when there exist (a) an admissible fixed point of f_- and g_- (black dot), and a virtual fixed point of f_+, g_+ (small circle), and (b) an admissible fixed point of f_+ and g_+ (black dot), and a virtual fixed point of f_-, g_- (small circle)

- birth of two admissible equilibrium points;
- birth of two virtual equilibrium points;
- birth of an admissible and a virtual equilibrium.

Thus it would appear that twelve distinct scenarios are possible.

However, the number of existing scenarios will be less then that and it is limited by the fact that at the points of intersection of $\mathcal{M}_+^\varepsilon$ and $\mathcal{M}_-^\varepsilon$ with Σ the vector fields have the same sign. In other words we will not encounter small amplitude oscillations between $\mathcal{M}_+^\varepsilon$ and $\mathcal{M}_-^\varepsilon$ in the neighborhood of the origin, and the flow will either cross the switching manifold and diverge from the origin or it will reach an equilibrium point existing in the $\mathcal{O}(\varepsilon)$ neighborhood of the origin.

To show this let us calculate the $(\dot{x},\, \dot{y})$ on the slow manifolds about the origin for vector fields $(f_+,\ g_+)$, and $(f_-,\, g_-)$ respectively. If it can be shown that $\dot{x}$ and $\dot{y}$ can take the opposite signs on the slow manifolds in some small neighborhood of the origin then there is a possibility of oscillations across Σ. About the origin $\dot{y}_\pm = \varepsilon d$ and $\dot{x}_\pm = BC_\pm^{-1}\varepsilon d$. Therefore, both $\dot{y}_\pm$ and $\dot{x}_\pm$ are characterized by the same sign on Σ and hence small scale oscillations across Σ cannot occur.

4.2.1 Phase portraits for Case I ($c_+BC_+^{-1} + b > 0$ and $c_-BC_-^{-1} - b > 0$)

In the current case there are two scenarios possible: (i) for $d > 0$ there exist an admissible fixed point of f_-, g_- and a virtual fixed point of f_+, g_+ (see Fig. 2(a)) or (ii) for $d < 0$ there exist an admissible fixed point of f_+ and g_+ and a virtual fixed point of f_-, g_- (see Fig. 2(b)). Note that this follows from (36) under our assumption that $B > 0$. In the former of these two cases the flow moves to the right across Σ and in the latter to the left across Σ.

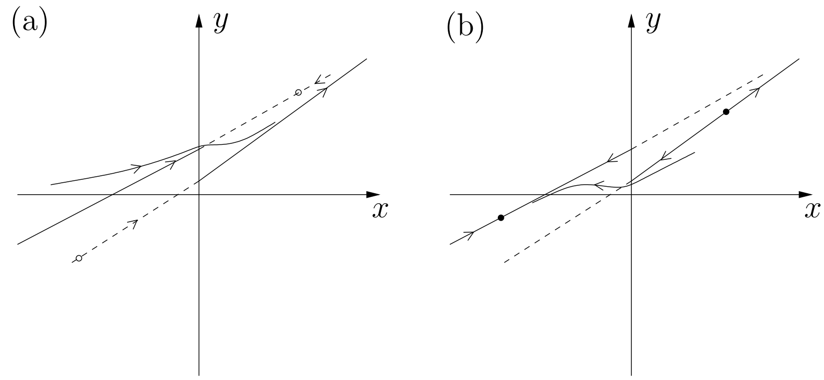

Fig. 3. Phase portraits of the slow fast system (33) and (35) about the origin for $\varepsilon > 0$ in the case when there exist (a) no admissible fixed points of f_-, g_- and f_+, g_+, and (b) there exist an admissible fixed point of f_+, g_+ and of f_-, g_- (an attracting fixed point on the left and a saddle point on the right)

4.2.2 Phase portraits for Case II ($c_+BC_+^{-1} + b > 0$ and $c_-BC_-^{-1} + b < 0$)

In the current case there are two scenarios possible: (i) the existence of two virtual fixed points of f_-, g_- and of f_+, g_+ for $d > 0$ (see Fig. 3(a)) or (ii) there exist two admissible fixed points, one of f_+, g_+ and the other of f_-, g_- for $d < 0$ (see Fig. 3(b)). In the former of these two cases the flow moves to the right across Σ and in the latter there exist an attracting fixed point on $\mathcal{M}_-^\varepsilon$ and a saddle point on $\mathcal{M}_+^\varepsilon$.

4.2.3 Phase portraits for Case III ($c_+BC_+^{-1} + b < 0$ and $c_-BC_-^{-1} + b < 0$)

In the current case there are two scenarios possible: (i) the existence of an admissible fixed point of f_-, g_- and of a virtual fixed point of f_+, g_+ for $d < 0$ (see Fig. 4(a)) or (ii) there exist an admissible fixed points of f_+, g_+ and a virtual fixed point of f_-, g_- for $d > 0$ (see Fig. 4(b)). In either case the admissible fixed point is a local attractor. In the former of these two cases the flow moves to the left and in the latter to the right across Σ.

4.2.4 Phase portraits for Case IV ($c_+BC_+^{-1} + b < 0$ and $c_-BC_-^{-1} + b > 0$)

This case is equivalent to case II. Namely, for $d > 0$ there exist an attracting fixed point on the right and a saddle point on the left of the switching manifold and the flow, for points sufficiently close to the switching surface, moves to the right across Σ; or for $d < 0$ there are only virtual fixed points in the neighborhood of the origin and the flow moves to the left across Σ

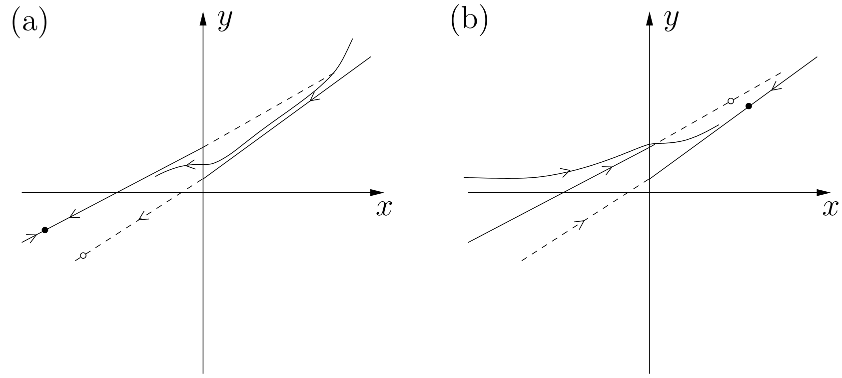

Fig. 4. Phase portraits of the slow fast system (33) and (35) about the origin for $\varepsilon > 0$ in the case when there exist (a) an admissible fixed points of f_-, g_- and a virtual fixed point of f_+, g_+, and (b) an admissible fixed point of f_+, g_+ and a virtual fixed point of f_-, g_-

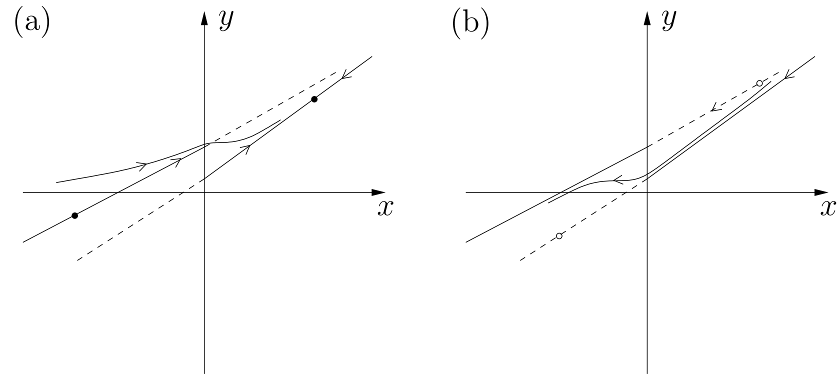

Fig. 5. Phase portraits of the slow fast system (33) and (35) about the origin for $\varepsilon > 0$ in the case when there exist (a) an admissible fixed points of f_-, g_- and f_+, g_+ (an attracting fixed point on the right and a saddle point on the left), and (b) only virtual fixed points of f_+, g_+ and of f_-, g_-

5 Example: Box model of thermohaline circulation

In the following section we will apply our results to analyse a mathematical model of thermohaline circulation. The thermohaline circulation (or 'conveyor belt') in the ocean is a current which transports warm water near the surface from equatorial to polar regions, and cold water at deeper levels back from the polar regions to the equator. It is driven by heat (the warmer water cools and then due to greater density sinks as it reaches the poles) and salt (surface water becomes more salty at the equator as water is removed by evaporation due to the greater heat) which makes it heavier and allows less salty water to rise). Thermohaline circulation is a major source of heat transfer, and it has been disrupted in the past, leading to major climate change, and it may be that the effects of current climate change could change the circulation pattern again. Investigation of this has led back to the 'box' models of circulation developed by Stommel [16]. In these models the polar region is described by one well-

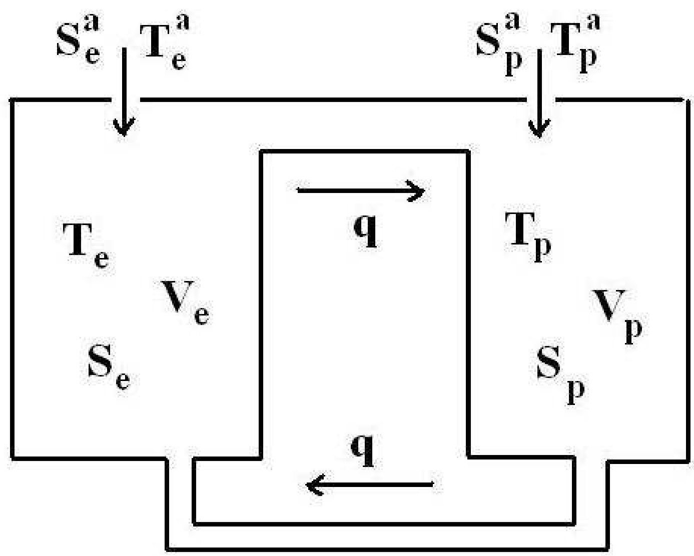

Fig. 6. Schematic diagram of the box model. Variables with subscripts e are in the low latitude (equatorial) region and variables with subscripts p are in the higher latitude (polar) region (after Dijkstra [15]).

mixed box with temperature T_p and salinity S_p, whilst the equatorial region is represented by another well-mixed box with temperature T_e and salinity S_e as shown in Figure 6. These boxes are connected near the surface and at depth by tubes which allow a flux q to flow between the boxes which depends upon the temperature and salinity differences between the boxes. Stommel [16] made the ansatz that the flux is dominated by the density difference between the regions,

$$q = \gamma \left(\frac{\rho_p - \rho_e}{\rho_0} \right),$$

where ρ_p and ρ_e are the polar and equatorial densities of the water, given in terms of reference temperatures, salinity and density T_0, S_0 and ρ_0 by

$$\rho = \rho_0(1 - \alpha_T(T - T_0) + \alpha_S(S - S_0)).$$

Thus

$$q = \gamma \left(\alpha_T(T_e - T_p) - \alpha_S(S_e - S_p) \right). \tag{37}$$

Following Stommel and Dijkstra [15], assume that heat is added to the polar (resp. equatorial) box at a rate T_p^a (resp. T_e^a) from the atmosphere, with $T_e^a - T_p^a > 0$, and that salinity is increased at the equator (evaporation) and decreased at the pole (precipitation) at rates S_e^a and S_p^a with $S_e^a - S_p^a > 0$.

Then the model is defined by four differential equations:

$$\begin{aligned}
V_e \tfrac{d}{dt} T_e &= C_e^T (T_e^a - T_e) + |q|(T_p - T_e),\\
V_p \tfrac{d}{dt} T_e &= C_p^T (T_p^a - T_p) + |q|(T_e - T_p),\\
V_e \tfrac{d}{dt} S_e &= C_e^S (S_e^a - S_e) + |q|(S_p - S_e),\\
V_p \tfrac{d}{dt} S_e &= C_p^S (S_p^a - S_p) + |q|(S_e - S_p).
\end{aligned} \tag{38}$$

It is standard to assume that the relaxation rates for the temperature are equal and constant, so $C_e^T/V_e = C_p^T/V_p = R_T$ and similarly for salinity $C_e^S/V_e = C_p^S/V_p = R_S$. With this simplifying assumption the equations can be combined to obtain two differential equations for the temperature difference $\Delta T = T_e - T_p$, and the salinity difference $\Delta S = S_e - S_p$ as

$$\begin{aligned}
\tfrac{d}{dt}\Delta T &= R_T([T_e^a - T_a^p] - \Delta T) - 2|Q|\Delta T\\
\tfrac{d}{dt}\Delta S &= R_S([S_e^a - S_a^p] - \Delta S) - 2|Q|\Delta S
\end{aligned}, \tag{39}$$

where

$$Q = \gamma(\alpha_T \Delta T - \alpha_S \Delta S). \tag{40}$$

Now define $\Delta T^a = T_e^a - T_p^a$ and $\Delta S^a = S_e^a - S_p^a$, and rescale the equations by setting

$$x = \frac{\Delta T}{\Delta T^a},\ y = \frac{\alpha_S \Delta S}{\alpha_T \Delta T^a},\ \tau = R_S t \tag{41}$$

(this is a slightly different scaling than that used in [15], and will make it possible to use singular perturbation theory a little later; the same idea is used by Berglund and Gentz [17] on a slightly different model) giving

$$\begin{aligned}
\tfrac{d}{d\tau} x &= \tfrac{R_T}{R_S}(1 - x) - A|x - y|x,\\
\tfrac{d}{d\tau} y &= \mu - (1 + A|x - y|)y,
\end{aligned} \tag{42}$$

where

$$\mu = \frac{\alpha_S \Delta S^a}{\alpha_T \Delta T^a},\quad A = \frac{2\gamma \alpha_T \Delta T^a}{R_S}. \tag{43}$$

To understand the behaviour of this system make one further (reasonable) assumption:

$$R_S \ll R_T \tag{44}$$

so that $\varepsilon = R_S/R_T$ is a small parameter. Then (42) can be rewritten as

$$\begin{aligned}
\varepsilon \dot{x} &= (1 - x) - \varepsilon A|x - y|x\\
\dot{y} &= \mu - (1 + A|x - y|)y
\end{aligned} \tag{45}$$

where the dot denotes differentiation with respect to τ.

Equation (45) is almost in the form analyzed in previous sections, but to be able to apply the results of Sec. 4 we will make a further transformation to bring the switching surface to the coordinate axis: set

$$u = x - y, \quad v = 1 - y$$

so $y = 1 - v$ and $x = 1 - v + u$. In terms of these variables (45) becomes

$$\begin{aligned} \varepsilon \dot{u} &= v - u + \varepsilon(1 - \mu - v - A|u|u), \\ \dot{v} &= 1 - \mu - v + A|u|(1 - v). \end{aligned} \tag{46}$$

This is now precisely the form considered in Sec. 4.1 with $C_\pm = 1$, $B = 1$ and $D = 1$. We find that the slow manifolds up to and including terms of order $\mathcal{O}(\varepsilon^3)$ are given by

$$u_+(v) = v - \varepsilon A v + \varepsilon^2(A(1-\mu) + Av + 2A^2 v) + \mathcal{O}(\varepsilon^3), \tag{47}$$

$$u_-(v) = v + \varepsilon A v + \varepsilon^2(-A(1-\mu) + Av + 2A^2 v) + \mathcal{O}(\varepsilon^3). \tag{48}$$

Note that, in the current case the size of the discontinuity across the switching surface is not of $\mathcal{O}(\varepsilon)$ but is of $\mathcal{O}(\varepsilon^2)$ (provided that $\mu \neq 1$). We note that h_y in (22) is naught. Moreover, $\alpha_1^* = \beta_1^*$ since $f_\pm^1 = 1 - \mu - v$ at $(u^*, v^*) = (0\ 0)$ and thus the discontinuity across Σ is of $\mathcal{O}(\varepsilon^2)$.

If, on the other hand $\mu = 1$, then our system exhibits an equilibrium point on the switching surface and the discontinuity is of $\mathcal{O}(\varepsilon^3)$.

Using equation (34) we can compute $u_\pm(v)$ to leading order by noting that $a = g(0, 0, \varepsilon) = \dot{v}(0, 0, \varepsilon) = 1 - \mu$. Thus we obtain $u_\pm(v) = v - \varepsilon(1-\mu) + \varepsilon(1-\mu) = v$, which to leading order agrees with (47) and (48). Finally, we compute the direction of the flow at the two intersection points of the slow manifold with the switching surface. These points are given by functional expressions (48) and (47), Thus we have to compute $\dot{u}_\pm(v_i)$ and $\dot{v}_\pm^i$, where v^i denotes the value of the v component for each of these two points. We note that $v_\pm^i$ are an $\mathcal{O}(\varepsilon^2)$ away from the origin. In our case, to leading order, we find $\dot{u}_\pm^i = \dot{v}_\pm^i$ and $\dot{u}_\pm^i = 1 - \mu$. If $1 - \mu$ is positive then the flow across the switching surface is to the right and upwards along the increasing values of u. Otherwise it is to the left and downwards along the decreasing values of u.

We have to consider now the final scenario which occurs when $\mu - 1 = 0$. This is the case presented in Sec. 4.2. For $\mu - 1 = 0$ the reduced system (46), as well as the full system with non-zero ε, exhibit an equilibrium on the switching surface. Depending on the value of A this equilibrium can be either:

- for $A \in (-1,\ 1)$ a stable fixed point;
- for $A \in (-\infty,\ -1) \cup (1,\ \infty)$ a saddle point.

Since the position of the equilibrium is independent of ε when $\mu = 1$ then there is no change in qualitative dynamics when the full system is considered. The slow manifolds $\mathcal{M}_{\pm}^{\varepsilon}$ join the switching surface at the origin, at the equilibrium point.

However, we may consider small size perturbations of $\mu - 1$ about $\mu = 1$ to determine the phase portraits of the slow-fast system (46). In this setting we can use the analysis from Sec. 4.2 with $d\varepsilon = 1 - \mu$ in equation (35). Then in the nomenclature of Sec. 4.2 we have to check the conditions on the signs of $c_+ BC_+^{-1} + b$ and $c_- BC_-^{-1} + b$. We have that $c_+ = A$, $c_- = -A$, $b = -1$, $C_{\pm} = 1$ and $B = 1$. Therefore our conditions simplify to determining the signs of $A - 1$ and $-A - 1$. Clearly, depending on A, different scenarios, as enumerated in Sec. 4.2 may take place:

(1) if $-1 < A < 1$, then $A - 1 < 0$ and $-A - 1 < 0$, and we have two possible scenarios as depicted in Fig. 4. If $1 - \mu > 0$ then the system crosses the switching surface along the increasing values of u and tends towards the attractor on $u_+(v)$ which corresponds to the case presented in Fig. 4(b). On the other hand, if $1 - \mu < 0$, then the system crosses the switching surface along the decreasing values of u and tends towards the attractor on $u_-(v)$, which corresponds to the case presented in Fig. 4(a);
(2) if $-\infty < A < -1$, then $A - 1 < 0$ and $-A - 1 > 0$, and we have two possible scenarios as depicted in Fig. 5. If $1 - \mu > 0$ then there exists and attracting fixed point on u_+ and an unstable fixed point on u_-, see Fig. 5(a). On the other hand, if $1 - \mu < 0$, then there no equilibrium points in some small neighborhood of the origin and the flow moves across the switching surface, see Fig. 5(b);
(3) if $1 < A < \infty$, $A - 1 > 0$ and $-A - 1 < 0$, and we have two possible scenarios as depicted in Fig. 3. If $1 - \mu > 0$ there are no fixed points in some small neighborhood of the origin, see Fig. 3(a), and if $1 - \mu < 0$ then there exists and attracting fixed point on u_- and an unstable fixed point on u_+, see Fig. 3(b).

The scenarios occurring under the variation of μ through 1 for $A \in (-\infty,\ 1) \cup (1,\ \infty)$ correspond to the non-smooth equivalent of a saddle-node bifurcation.

Having established the dynamics of the system across the switching manifolds for different values of μ and A we can complete the investigations of our system by considering other invariant sets existing away from the switching manifold. Since the remaining analysis is standard and we wish to restrict ourselves to parameter values coming from our modeling we return to (45) to complete the analysis. In what follows we consider positive A only; these values of A are feasible physically - see (43). We first look at the existence of fixed points on the slow manifold $x = 1$ (this is an approximate expression for the slow

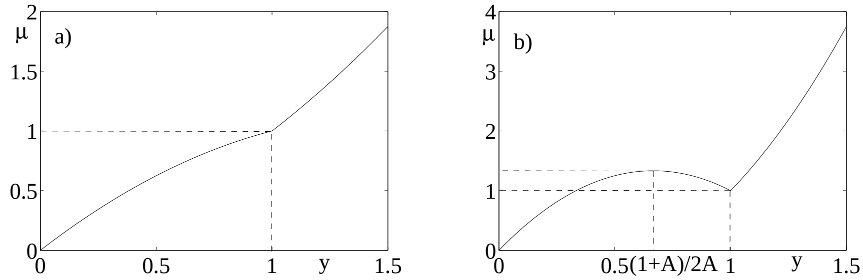

Fig. 7. Sketch of the graphs of the right hand side of (49) for (a) $A < 1$; and (b) $A > 1$.

manifold up to order $\mathcal{O}(\varepsilon)$) of (45). That is we will analyze

$$\mu = \begin{cases} (1+A)y - Ay^2 & \text{for} \quad y < 1, \\ (1-A)y + Ay^2 & \text{for} \quad y > 1. \end{cases} \tag{49}$$

If $0 < A < 1$ then the right hand side of (45) is a monotonic increasing function with a discontinuity in the derivative at $y = 1$ (see Fig. 7 a)), so for each value of μ there is a corresponding fixed point which is stable.

The case $A > 1$ is more interesting. In this case the turning point of the quadratic defined in $y < 1$ is $y = (1 + A)/2A$, where the function takes its maximum value $\mu = (1 + A)^2/4A$. Since this turning point now lies in $y < 1$, the graph of (49) has a turning point in $y < 1$ and the decreasing branch attaches to the increasing branch of the parabola in $y > 1$ at $y = 1$, at which the right hand side of (49) takes the value of unity. Thus there are three cases (imagine moving a horizontal line of constant μ up or down in Figure 7 b)):

- if $\mu < 1$ the system has one stable solution in $y < 1$;
- if $1 < \mu < (1 + A)^2/4A$ there are three solutions: two of these are stable, one in $y < 1$ and the other in $y > 1$;
- if $\mu > 1$ then there is a single solution with $y > 1$.

The bifurcation at $\mu = 1$ is a non-smooth version of the saddle-node bifurcation, creating a pair of stable and unstable solutions and it has been discussed in detail in the (u, v) co-ordinates (see cases 2 and 3 on the previous page); the bifurcation at $\mu = (1 + A)^2/4A$ is a standard saddle-node bifurcation. The stability diagram is usually described as in Figure 8, which is essentially Figure 7(b) turned on its side, and shows the evolution of the fixed points as a function of μ. Current estimations show that the ocean parameters are such that we lie on the upper branch of the stable solutions in Figure 8. This suggests two sources for concern: if the parameters are in the (middle) bistable region, then a perturbation of initial conditions, i.e. some extraneous effect not described by the box model, could push us onto the weaker lower stable solution; or the parameter μ may be changing in such a way that it approaches

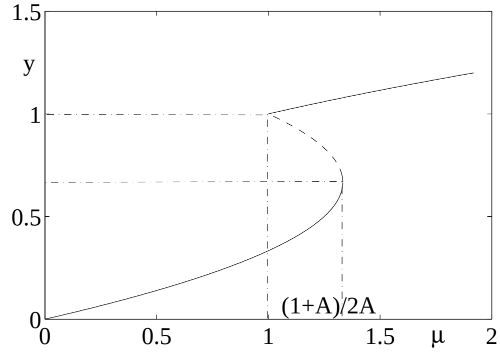

Fig. 8. Fixed points of system (45) on the slow manifold $x = 1$ approximated to $\mathcal{O}(\varepsilon)$ for $A > 1$. Note the existence of three equilibrium states for $1 > \mu > (1 + A)/2A$ which is the region of bi-stability. The dashed line denotes the unstable and the solid line the stable equilibrium points, and the dash-dotted lines denote the points where the saddle-node bifurcations occur.

$\mu = (1 + A)^2/4A$ at which point the system moves dramatically to the stable lower solution.

Note that the interpretation of solutions relies on the direction of the flow q in (37), and in terms of the variables x and y defined in (41) this becomes proportional to $x - y$, i.e. to $1 - y$ on the slow manifold. The concern for the implications of climate change is that if $A > 1$ and $1 < \mu < (1 + A)^2/(4A)$, a stable solution with $q > 0$ can coexist with a stable solution with $q < 0$, indicating the possibility of flow reversal.

6 Higher-dimensional slow-fast systems

We wish to conclude the paper with a discussion on the topology of the slow manifold in the case when the dimension of the slow subsystem is n. We will then use a 3-dimensional piecewise-smooth system with the slow dynamics being two dimensional to illustrate the implications of phase space topology on the existence and stability of an isolated hyperbolic limit cycle present in the reduced system.

6.1 Phase space topology

Consider system (1) and (2) assuming that $\mathbf{y} \in \mathbb{R}^n$. The description of phase space is equivalent to the one presented in Sec. 2 but the topology is embedded in $\mathbb{R}^{n+1}$ dimensional phase space (differentiability of $f\pm$ and $g_\pm$ is assumed). In what follows we will use the notation as introduced in Sec. 3. Thus $\mathcal{M}_\pm$

denote the slow manifolds of the reduced system in G_+ and G_- respectively. Similarly $\mathcal{M}^{\varepsilon}_{\pm}$ denote the slow manifolds of the full system in G_+ and G_- respectively. Manifolds $\mathcal{M}_{\pm}$ are defined using relations $f_{\pm}(x,\,\mathbf{y};\,0) = 0$ in $\mathbb{R}^{n+1}$ dimensional phase space. In the region of interest equations $f_+(x,\,\mathbf{y};\,0) = 0$ and $f_-(x,\,\mathbf{y};\,0) = 0$ can be solved for x as a function of y giving $x = \alpha_0(\mathbf{y})$ and $x = \beta_0(\mathbf{y})$ respectively. Since $f_+(x,\,\mathbf{y};\,0) = f_-(x,\,\mathbf{y};\,0)$ on the switching surface these manifolds are continuous but non-differentiable on Σ and $\alpha_0(\mathbf{y}) = \beta_0(\mathbf{y})$ on Σ. In other words, the vectors normal to $\mathcal{M}_{\pm}$ on Σ, are such that $\nabla f_+(x,\,\mathbf{y};\,0) \neq \nabla f_-(x,\,\mathbf{y};\,0)$ on Σ.

Let $f_- = f_+ = f = f^{(0)} + \varepsilon f^{(1)} + \mathcal{O}(\varepsilon^2)$ and $\mathbf{g}_- = \mathbf{g}_+ = \mathbf{g} = \mathbf{g}^{(0)} + \varepsilon\mathbf{g}^{(1)} + \mathcal{O}(\varepsilon^2)$ for $(x,\,\mathbf{y}) \in \Sigma$ where $\mathbf{g} : \mathbb{R}^{n+1} \mapsto \mathbb{R}^n$ and $f : \mathbb{R}^{n+1} \mapsto \mathbb{R}$.

Let us linearize (2) (for $\mathbf{y} \in \mathbb{R}^n$) about some point $(\alpha_0(\mathbf{y}_0),\,\mathbf{y}_0) \in \Sigma$ and compute the functional expressions for the slow manifold in the full system up to and including terms of $\mathcal{O}(\varepsilon)$. That is we seek an expression equivalent to (34) for $\mathbf{y} \in \mathbb{R}^n$. Thus to leading order we have

$$\varepsilon\dot{x} = \begin{cases} f_+(x_0,\mathbf{y}_0) - C_+(x - x_0) + \partial_y f_+(\mathbf{y} - \mathbf{y}_0) + D\varepsilon, & \text{if,} \quad h(x,\mathbf{y}) \geq 0 \\ f_-(x_0,\mathbf{y}_0) - C_-(x - x_0) + \partial_y f_-(\mathbf{y} - \mathbf{y}_0) + D\varepsilon, & \text{if} \quad h(x,\mathbf{y}) < 0, \end{cases} \tag{50}$$

where $C_{\pm}$ are arbitrary but positive constants by (3) and $\partial_y f$ is a gradient vector to f when treating the fast variable 'x' as a constant. From (50) we have that the slow manifold $\mathcal{M} = \mathcal{M}_+ \bigcup \mathcal{M}_-$ of the reduced system across the switching surface $\Sigma := \{h(x,\,\mathbf{y}) = 0\}$ is approximated by the functional expressions

$$x_+(\mathbf{y}) = x_0 + C_+^{-1} f_+(x_0,\,\mathbf{y}_0) + C_+^{-1}\langle \partial_y f_+, (\mathbf{y} - \mathbf{y}_0)\rangle \tag{51}$$

and

$$x_-(\mathbf{y}) = x_0 + C_-^{-1} f_-(x_0,\,\mathbf{y}_0) + C_-^{-1}\langle \partial_y f_-, (\mathbf{y} - \mathbf{y}_0)\rangle, \tag{52}$$

where $(x_0,\,\mathbf{y}_0) \in \Sigma$. By the definition of the slow manifold of the reduced system $f_+(x_0,\,\mathbf{y}_0) = f_-(x_0,\,\mathbf{y}_0) = 0$ for $(x_0,\,\mathbf{y}_0) \in \mathcal{M}$. Thus

$$x_+^{(0)}(\mathbf{y}) = x_0 + C_+^{-1}\langle \partial_y f_+, (\mathbf{y} - \mathbf{y}_0)\rangle \tag{53}$$

and

$$x_-^{(0)}(\mathbf{y}) = x_0 + C_-^{-1}\langle \partial_y f_-, (\mathbf{y} - \mathbf{y}_0)\rangle. \tag{54}$$

Using (50) we can find the approximate expression for the slow manifold of the full slow fast system. We assume without loss of generality that $g_{\pm}(x,\,\mathbf{y},\varepsilon) \approx \mathbf{a} \neq 0$ for all $(x,\,\mathbf{y})$ in a sufficiently small neighborhood of $(x_0,\,\mathbf{y}_0)$, where $\mathbf{a}$ is a constant vector. Then

$$x_+(\mathbf{y}) = x_0 + C_+^{-1}\langle \partial_y f_+, (\mathbf{y} - \mathbf{y}_0)\rangle + \varepsilon(C_+^{-1} D - C_+^{-2}\langle \partial_y f_+, \mathbf{a}\rangle) \tag{55}$$

and

$$x_-(\mathbf{y}) = x_0 + C_-^{-1}\langle \partial_y f_-, (\mathbf{y}-\mathbf{y}_0)\rangle + \varepsilon(C_-^{-1}D - C_-^{-2}\langle \partial_y f_-, \mathbf{a}\rangle). \tag{56}$$

Let us suppose that $(x_0,\, \mathbf{y}_0) = \mathbf{0}$, which can be assumed without loss of generality. Then by the continuity of f_- and f_+ across Σ for any $(x,\, \mathbf{y}) \in \Sigma$ sufficiently close to $\mathbf{0}$ by the continuity of $f(x,\, \mathbf{y}; \varepsilon)$ on Σ we require

$$C_+ h_x^{-1}\mathbf{h}_\mathbf{y} + \partial_y f_+ = C_- h_x^{-1}\mathbf{h}_\mathbf{y} + \partial_y f_- \tag{57}$$

where subscripts x and y denote differentiation with respect to x and $\mathbf{y}$ variables respectively and all the quantities are evaluated at $\mathbf{0}$.

Let us now calculate the points of intersections of $\mathcal{M}_\pm^\varepsilon$ with Σ, say $\mathbf{y}_\pm^{in}$. We know that

$$h(x_\pm^{in},\, \mathbf{y}_\pm^{in}) = 0. \tag{58}$$

Expanding (58) in $x_\pm^{in}$ and $\mathbf{y}_\pm^{in}$ to leading order about $\mathbf{0}$ gives

$$h_x x_\pm^{in} + \mathbf{h}_\mathbf{y}\mathbf{y}_\pm^{in} \approx 0. \tag{59}$$

Using (55) for x_+^{in} we have

$$h_x \left(C_+^{-1}\langle \partial_y f_+ \mathbf{y}_+^{in} + \varepsilon(C_+^{-1}D - C_+^{-2}\langle \partial_y f_+, \mathbf{a}\rangle) \right) + \mathbf{h}_\mathbf{y}\mathbf{y}_+^{in} + \mathcal{O}(\varepsilon^2) = 0.$$

Rearranging gives

$$\mathbf{y}_+^{in} = -A^{-1}\mathbf{h}_\mathbf{y}^\mathbf{T} h_x k\varepsilon + \mathcal{O}(\varepsilon^2), \tag{60}$$

where

$$A^{-1} = \left[\mathbf{h}_\mathbf{y}^\mathbf{T}\left(h_x C_+^{-1}\partial_y f_+ + \mathbf{h}_\mathbf{y}\right)\right]^{-1}, \qquad k = C_+^{-1}D - C_+^{-2}\langle \partial_y f_+, \mathbf{a}\rangle.$$

Similarly

$$\mathbf{y}_-^{in} = -\bar{A}^{-1}\mathbf{h}_\mathbf{y}^\mathbf{T} h_x \bar{k}\varepsilon + \mathcal{O}(\varepsilon^2), \tag{61}$$

where

$$\bar{A}^{-1} = \left[\mathbf{h}_\mathbf{y}^\mathbf{T}\left(h_x C_-^{-1}\partial_y f_- + \mathbf{h}_\mathbf{y}\right)\right]^{-1}, \qquad \bar{k} = C_-^{-1}D - C_-^{-2}\langle \partial_y f_-, \mathbf{a}\rangle.$$

Generically, unless some nonstandard cancelation occurs $A^{-1} \neq \bar{A}^{-1}$ and $k \neq \bar{k}$. Thus $\mathbf{y}_\pm^{in}$ are $\mathcal{O}(\varepsilon)$ distance away on Σ, and the $\mathcal{O}(\varepsilon)$ discontinuity of $\mathcal{M}_\pm^\varepsilon$ on Σ is preserved in the multidimensional case.

Let us now determine if there is a possibility of boundary oscillations between $\mathcal{M}_-^\varepsilon$ and $\mathcal{M}_+^\varepsilon$ across the switching surface Σ. To this aim we calculate the derivative $\frac{\mathrm{d}h}{\mathrm{d}t}$ at the points of intersection of $\mathcal{M}_\pm^\varepsilon$ with Σ. If both these derivatives are characterized by the same sign then we cannot observe the boundary layer oscillations since then the system trajectories move across Σ

and approach the slow manifold $\mathcal{M}^{\varepsilon}_{\pm}$ exponentially fast after crossing Σ. We have:

$$\frac{\mathrm{d}h}{\mathrm{d}t}(\mathbf{y}=\mathbf{y}^{in}_{+}) = h_x\frac{\mathrm{d}x}{\mathrm{d}y}\dot{\mathbf{y}} + h_y\dot{y} = h_x C_{+}^{-1}\langle \partial_y f_{+},\, \mathbf{a}\rangle + \langle h_y,\, \mathbf{a}\rangle \tag{62}$$

and

$$\frac{\mathrm{d}h}{\mathrm{d}t}(\mathbf{y}=\mathbf{y}^{in}_{-}) = h_x\frac{\mathrm{d}x}{\mathrm{d}y}\dot{\mathbf{y}} + h_y\dot{y} = h_x C_{-}^{-1}\langle \partial_y f_{-},\, \mathbf{a}\rangle + \langle h_y,\, \mathbf{a}\rangle, \tag{63}$$

where $(x_{+}(\mathbf{y}^{in}_{+}),\, \mathbf{y}^{in}_{+}) \in \Sigma \cup \mathcal{M}^{\varepsilon}_{+}$ and $(x_{-}(\mathbf{y}^{in}_{-}),\, \mathbf{y}^{in}_{-}) \in \Sigma \cup \mathcal{M}^{\varepsilon}_{-}$. Using (57) we can rewrite (64) as

$$\frac{\mathrm{d}h}{\mathrm{d}t}(\mathbf{y}=\mathbf{y}^{in}_{+}) = C_{+}^{-1}\left(h_x\langle \partial_y f_{-},\, \mathbf{a}\rangle + C_{-}\langle h_y,\, \mathbf{a}\rangle\right). \tag{64}$$

We now have to compare expressions (63) and (64). It can be easily shown that both these expressions are characterized by the same sign for all admissible values of the coefficients. Hence, small scale oscillations across the boundary Σ are not possible. This has further implications as to the qualitative dynamics of the slow-fast system (1) and (2) for $\mathbf{y} \in \mathbb{R}^n$. If a hyperbolic limit cycle exists in the reduced system then it will also exist in the full system and it will have the same stability properties – the change in the value of its Floquet multipliers is at most of $\mathcal{O}(\varepsilon)$.

We will illustrate this in the following section on a numerical example where the dimension of the slow subsystem is two.

6.2 Illustrative example

Consider a slow-fast system of the form

$$\dot{\mathbf{y}} = \begin{cases} y_1 - \omega y_2 - (x + y_2^2)y_1, \\ \omega y_1 + y_2 - (|y_1| + y_2^2)y_2, \end{cases}$$
$$\varepsilon\dot{x} = |y_1| - x \tag{65}$$

where $\mathbf{y} = (y_1,\, y_2)^T$. It is straightforward to verify that system (65) is continuous across the switching surface $\{y_1 = 0\}$. The slow dynamics of system (65) is based on the normal form for a supercritical Hopf bifurcation that allows to construct simple planar piecewise-continuous system which exhibits stable periodic orbits.

The reduced system for (65) with $\varepsilon = 0$ has $x = |y_1|$ and is hence

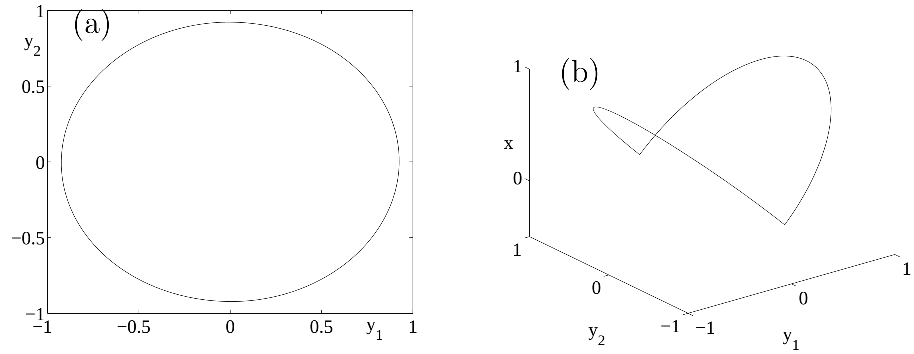

Fig. 9. A limit cycle of the reduced system (66); (a) in the projection onto slow variables $(y_1,\ y_2)$, and (b) in 3-D phase space. Note corner type singularity across the switching plane $\{y_1 = 0\}$.

$$\dot{\mathbf{y}} = \begin{cases} y_1 - \omega y_2 - (|y_1| + y_2^2)y_1, \\ \omega y_1 + y_2 - (|y_1| + y_2^2)y_2, \end{cases} \tag{66}$$

which is the normal form for a supercritical Hopf bifurcation in parameter regions where a stable periodic orbit exists and with one of the usual squared terms replaced by a modulus. The limit cycle in the projection onto slow variables is depicted in Fig. 9(a). It is characterized by one non-trivial Floquet multiplier $\mu = 0.13813$. The slow manifolds $\mathcal{M}_+$ and $\mathcal{M}_-$ are given by the functional expressions $x = -y_1$ and $x = y_1$ respectively. The corner type singularity is clearly visible across the switching surface $\{y_1 = 0\}$ in Fig. 9(b).

We should consider what is the effect of the applied singular perturbation on the existence and stability of the limit cycle. We first note that the limit cycle of the reduced system in the projection onto slow variables forms a differentiable closed curve since the right-hand side of (66) is continuous. Consider now the trajectories of (65) that are rooted on the slow manifold $\mathcal{M}_-^\varepsilon$ or $\mathcal{M}_+^\varepsilon$. Since $\mathcal{M}_\pm^\varepsilon$ are $\mathcal{O}(\varepsilon)$ distance away and the right-hand side of the slow subsystem of (65) is a $\mathcal{O}(\varepsilon)$ regular perturbation of (66) then the trajectories rooted on $\mathcal{M}_+^\varepsilon$ or on $\mathcal{M}_-^\varepsilon$ of the full system are $\mathcal{O}(\varepsilon)$ distance away from those of the reduced system up to the point of intersection with the switching surface. We established earlier that there cannot be any small boundary layer oscillations between $\mathcal{M}_\pm^\varepsilon$ since the direction of the flow at the intersection between $\mathcal{M}_+^\varepsilon$ and Σ, and $\mathcal{M}_-^\varepsilon$ and Σ are the same. This implies further that the trajectories starting on either $\mathcal{M}_-^\varepsilon$ or $\mathcal{M}_+^\varepsilon$ and crossing Σ must tend to $\mathcal{M}_-^\varepsilon$ or $\mathcal{M}_+^\varepsilon$ exponentially fast and by the continuity of the vector fields, in the projection onto slow dimensions the trajectories of the full system cannot cross. Moreover, since the discontinuity in the slow manifold $\mathcal{M}_-^\varepsilon \cup \mathcal{M}_+^\varepsilon$ is of an $\mathcal{O}(\varepsilon)$ the perturbation to the trajectories induced by the crossing in relation to those of the reduced system is bounded by the $\mathcal{O}(\varepsilon)$. Thus, trajectories rooted on the slow manifold of the full system can be seen as $\mathcal{O}(\varepsilon)$ continuous perturbations of the trajectories of the reduced system.

Therefore for sufficiently small ε if a hyperbolic limit cycle exists in (66) then it must also exist in (65). Let us now consider the effect of the singular perturbation on the stability of the limit cycle.

To determine if there can be any change in the stability properties of the limit cycle we consider the solutions of the variational equation for trajectories on $\mathcal{M}_{\pm}^{\varepsilon}$. These will be ε close to those given by the solution of the variation equation for trajectories on $\mathcal{M}_{\pm}$. The fact that there is a discontinuity across the switching surface adds additional near-identity correction to solutions of the variational equations for trajectories starting on either $\mathcal{M}_{-}^{\varepsilon}$ and $\mathcal{M}_{+}^{\varepsilon}$ and switching to a distinct flow across the switching surface. Therefore the monodromy matrix [18] obtained from the composition of the solutions of the variational equations built about a limit cycle of the full system (65) restricted to the projection onto slow variables will be a $\varepsilon-$perturbation of the monodromy matrix of the reduced system. Since the limit cycle of the reduced system is hyperbolic the characteristic equation of the monodromy matrix is characterized by two separate roots and $\mathcal{O}(\varepsilon)$ perturbation to the monodromy matrix translate onto $\mathcal{O}(\varepsilon)$ perturbation of the characteristic equation and on $\mathcal{O}(\varepsilon)$ perturbation of the roots. It then follows that the Floquet multipliers of the full system will be at most $\mathcal{O}(\varepsilon)$ distance away from the Floquet multipliers of the reduced system.

From the above, using the continuity argument, it then follows that for sufficiently small $\varepsilon > 0$ a hyperbolic limit cycle present in the reduced system will exist also in the full system and will preserve its stability properties. There will be $\mathcal{O}(\varepsilon)$ jump in the value of the non-trivial Floquet multiplier upon switching on ε to a positive value.

The discontinuity in a slow manifold across the switching surface Σ implies further that the limit cycle present in the full system no longer exhibits a corner type singularity when Σ is crossed; the trajectory evolves smoothly while moving from $\mathcal{M}_{+}^{\varepsilon}$ to $\mathcal{M}_{-}^{\varepsilon}$ across the switching surface while covering the distance of $\mathcal{O}(\varepsilon)$. The limit cycle of (65) with $\varepsilon = 0.01$ is depicted in Fig. 10. Note that indeed the corner type dynamics is smoothed out in the full system.

Finally, in Fig. 11 we are depicting the variation of the non-trivial Floquet multiplier calculated about a periodic point of the limit cycle as a function of the variable ε. Clearly there is a small jump in the value of the Floquet multiplier under the switching of ε to a positive value.

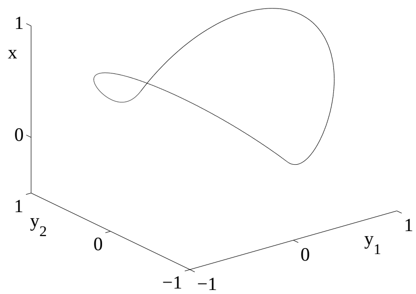

Fig. 10. A limit cycle of the slow-fast system (65) for $\varepsilon = 0.01$.

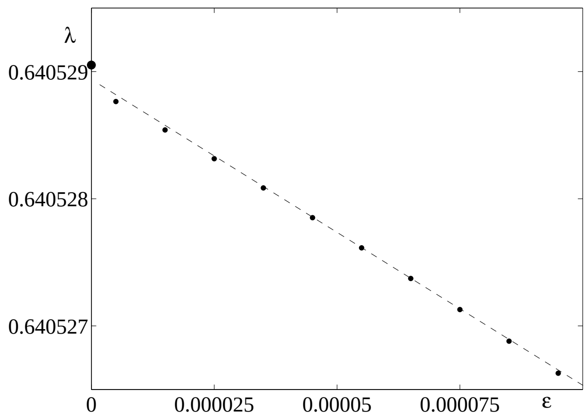

Fig. 11. Change in the value of the non-trivial Floquet multiplier of the reduced system (66) with $\omega = 20$ for $\varepsilon = 0$ (big black dot) against the full system (65) for $\varepsilon > 0$. Small black dots correspond to values of ε at which the value of the non-trivial Floquet multiplier was computed.

7 Conclusions

In the paper we consider the effects of singular perturbations on the dynamics of piecewise-smooth systems that are characterized by vector fields that have discontinuous jacobians across switching manifolds. We present a detailed analysis of planar systems that is systems with the slow and fast dynamics being one-dimensional. We show that the slow manifold of the reduced system is continuous but non-differentiable across the switching manifold. The slow manifold of the full system exhibits $\mathcal{O}(\varepsilon)$ discontinuity across the switching manifold. These results are generalized to $n+1$-dimensional systems – with the slow dynamics being one dimensional. In spite of the presence of the discontinuity across the switching surface small scale boundary oscillations between the slow manifolds are not possible. This implies that stable singular perturbations in the class of piecewise-smooth systems of interest cannot qualitatively alter system dynamics provided that no standard or discontinuity induced bifurcations take place in the systems.

Investigations of the qualitative dynamics in the case when the slow system has an equilibrium on the switching surface is also conducted for the planar case. Four distinct dynamic scenarios are found. This analysis is then used to investigate the dynamics of a planar piecewise-smooth slow-fast box model of thermohaline circulation. Combined effects of discontinuous nonlinearity and fast dynamics gave rise to a non-smooth equivalent of a fold scenario observed in the model.

Presented analysis opens up a number of important research questions. It has been shown that in the case when a planar Filippov type system exhibits so-called grazing-sliding scenario a stable singular perturbation applied to the system may result in the onset of micro-chaotic oscillations [14]. Hence grazing-sliding is not robust against stable singular perturbations. The question then arises if this would also be the case when grazing occurs in the absence of sliding which pertains to the class of systems considered here. Another important issue is the effect of singular perturbations when the reduced system exhibits an equilibrium on the switching manifold. The scenarios observed in the planar case will certainly be observed in higher dimensions but it is very likely that other cases will arise as well. This claim is justified by the fact that singular perturbations lead to boundary-equilibrium bifurcations – the reduced system has an equilibrium on the switching surface which is perturbed under the variation of ε to a positive value. Boundary-equilibrium bifurcations in three-dimensional piecewise-smooth flow lead, for instance, to a non-smooth equivalent of a Hopf bifurcation – a limit cycle which grows linearly in amplitude is born from an equilibrium colliding with the switching manifold [19]. Finally presented analysis rises a question whether singularly perturbed Filippov type systems with planar slow dynamics, in the absence of standard or discontinuity induced bifurcations, can exhibit dynamics qualitatively different from the one observed in the reduced model. In [13] it was shown that in the case when the switching function does not depend on the fast variable hyperbolic limit cycles present in the reduced system are also present in the full system preserving their stability properties.

Acknowledgements
Research partially funded by EPSRC grant EP/E050441/1 and the University of Manchester.

References

[1] S. Banerjee and G. Verghese. *Nonlinear Phenomena in Power Electronics.* IEEE press, New York, 2001.

[2] M. I. Feigin. *Forced Oscillations in Systems With Discontinuous Nonlinearities.* Nauka, Moscow, 1994. In Russian.

[3] K. Popp, N. Hinrichs, and M. Oestreich. Dynamical behaviour of friction oscillators with simultaneous self and external excitation. *Sadhana (Indian Academy of Sciences)*, 20:627–654, 1995.

[4] U. Galvanetto and S. R. Bishop. Dynamics of a simple damped oscillator undergoing stick-slip vibrations. *Meccanica*, 34:337–347, 2000.

[5] F. Peterka. Part 1: Theoretical analysis of n-multiple $(1/n)$-impact solutions. *CSAV Acta Technica*, 19:462–473, 1974.

[6] C. Budd, K.A. Cliffe, and F. Dux. The effect of frequency and clearance varions on one-degree of freedom impact oscillators. *J. Sound & Vibration*, 184, 1995.

[7] M. Oestreich, N. Hinrichs, K. Popp, and C. J. Budd. Analytical and experimental investigation of an impact oscillator. *Proceedings of the ASME 16th Biennal Conf. on Mech. Vibrations and Noise*, 1996.

[8] R.I. Leine. *Bifurcations in Discontinuous Mechanical Systems of Filippov-Type.* PhD thesis, Teknische Universiteit Eindhoven, The Netherlands, 2000.

[9] R.I. Leine and H. Nijmeijer. *Dynamics and Bifurcations of Non-Smooth Mechanical Systems*, volume 18 of *Lecture Notes in Applied and Computational Mechanics.* Springer–Verlag, Berlin Heidelberg, 2004.

[10] M. di Bernardo, C. J. Budd, A. R. Champneys, and P. Kowalczyk. *Piecewise-smooth Dynamical Systems: Theory and Applications.* Springer-Verlag, 2008.

[11] S. A. Lomov. *Introduction to the General Theory of Singular Perturbations.* American Mathematical Society, 1992.

[12] N. Fenichel. Geometric singular perturbation theory for ordinary differential equations. *Journal of Differential Equations*, 31:53–98, 1979.

[13] L. M. Fridman. Slow periodic motions with internal sliding modes in variable structire systems. *International Journal of Control*, 75:524–537, 2002.

[14] J. Sieber and P. Kowalczyk. Small-scale instabilities in dynamical systems with sliding. *Physica D*, 2009. Awaiting publications.

[15] H. A. Dijkstra. *Nonlinear Physical Oceanography.* Springer, Dordrecht, 2005.

[16] H. M. Stommel. Thermohaline convection with two stable regimes of flow. *Tellus*, 13:79–89, 1961.

[17] N. Berglund and B. Gentz. Metastability in simple climate models: pathwise analysis of slowly driven langevin equations. *Stochastics and Dynamics*, 2:327–356, 2002.

[18] R. Seydel. *From equilibrium to chaos. Practical bifurcation and stability analysis.* Springer-Verlag, New York, London, 1994.

[19] M. di Bernardo, A. Nordmark, and G. Olivar. Discontinuity-induced bifurcations of equlibria in piecewise-smooth and impacting dynamical systems. *Physica D*, 237:119–136, 2008.